JOURNAL OF EXPERIMENTAL AND THEORETICAL PHYSICS, 2024, Vol. 166, No. 3 (9), pp. 417–423

STATISTICAL, NONLINEAR, AND SOFT MATTER PHYSICS

EVOLUTION OF PLASMA RADIATION FROM BARRIER DISCHARGE IN LOW-PRESSURE NEON. ATOMIC SPECTRUM

© 2024 V. A. Ivanov*, Yu. E. Skoblo

St. Petersburg State University, 198504 St. Petersburg, Russia

**e-mail: v.a.ivanov@spbu.ru*

Received March 09, 2024
Revised April 21, 2024
Accepted April 21, 2024

Abstract. The results of a spectroscopic study of the plasma created by a barrier discharge in low-pressure neon are presented, reflecting the evolution of the mechanisms of population of excited levels of the Ne* atom and Ne^{+}* ion depending on the observation time relative to the beginning of the discharge. Analysis of the emission spectrum, correlated with measurements of the time dependences of the intensities of spectral lines, allows us to indicate four stages of spectrum evolution: direct population by electron impact in the active stage (discharge), followed by a stepwise population at its end with a transition, as the electron temperature relaxes, to recombination afterglow. The latter, depending on the gas pressure and the initial electron density, can also contain two stages – the initial one, with the predominance of the mechanism of collisional-radiative recombination of Ne^{++} and Ne^{+} ions with electrons as the source of population of all excited levels of the Ne^{+}* ion and neon atom observed in the experiment, and the final stage, the radiation in which is associated with the population of a limited group of levels due to the dissociative recombination of Ne_2^{+} molecular ions with electrons. The main attention in the work is paid to the population kinetics of the levels of configurations $2p^5 3p$ and $2p^5 4p$ of the neon atom.

Keywords: *dielectric barrier discharge, electron impact excitation, afterglow, collisional-radiative recombination, elementary processes, dissociative recombination*

DOI: 10.31857/S004445102409e13X

1. INTRODUCTION

This work is a continuation of a series of experiments [1–3] on using low-pressure dielectric barrier discharge (DBD) as a plasma source for studying elementary processes. Unlike traditional DBD, various variants of which have been successfully used in recent decades in many applications, such as creating active media for quantum generators [4] or efficient excimer radiation sources [5], we use periodic low-frequency discharge, in which the afterglow duration significantly exceeds the plasma creation stage time, allowing us to study electron-ion recombination mechanisms. In the radiation of such plasma, for the first time in experimental practice, an afterglow [1] associated with doubly charged ions was discovered, whose recombination with electrons radically changes the plasma spectrum in the near ultraviolet and allows estimating the process rate constant based on ionic line intensities [6]. The objective of this work was to determine, based on the analysis of spectra and time dependencies of spectral line intensities, the mechanisms of populating excited levels of neon atoms both in discharge and in the plasma decay stage.

2. EXPERIMENTAL SETUP AND RESULTS

The plasma creation method used in this work is described in detail in [1], so below we will focus only on those features that are important for this work. As in [1–3,6], we used a cylindrical discharge tube of

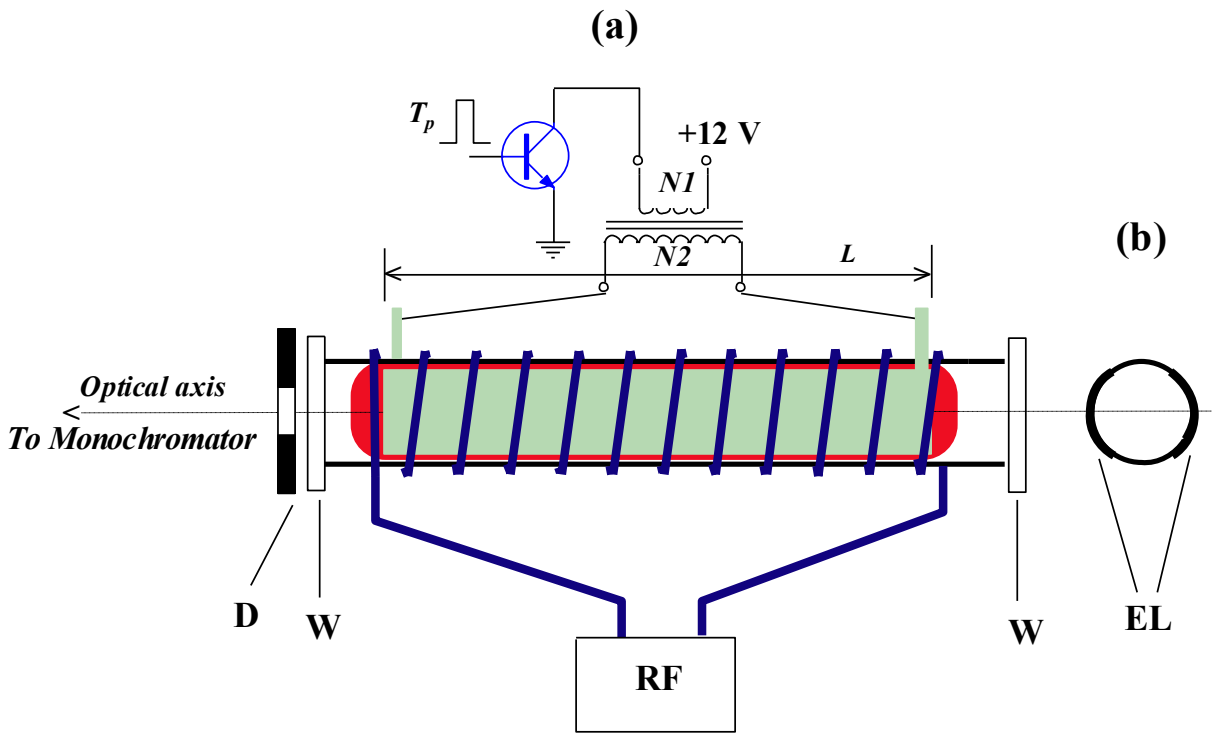

Fig. 1. a – Scheme of combining barrier and pulsed high-frequency discharges (RF) in a glass tube with 4 cm diameter. D – diaphragm with 5 mm diameter, W – quartz windows. b – Theplacement of DBD electrodes on the surface of the discharge tube

sufficiently large diameter (Fig.1) so that ambipolar diffusion would not be the main mechanism of plasma decay, at least in its initial phase. In the discharge scheme Fig. 1, the energy stored in the transformer when the transistor is open is transferred to the secondary winding at the end of im pulse T_p on its base, the voltage on the electrodes represents two half-waves of different polarity with slightly different (this difference depends on experimental conditions) amplitude and duration. Neon pressure P = 0.4 − 1.7 Torr. At such pressures, the use of barrier discharge compared to pulsed discharge between internal electrodes has the advantage of eliminating the problem of gas contamination by hard-to-remove electrode sputtering (mainly cathode). Moreover, the discharge of the used configuration creates an almost uniform plasma formation both along the longitudinal coordinate – the filamentary (streamer) nature of breakdown manifests, as experimental practice shows, at gas pressures $P \geqslant 15$ Torr – and along the radius [2].

The discharge frequency was set to 80 or 500 Hz depending on the studied stage.

Light fluxes were recorded using the multi-channel photon counting method with a time channel width of 40 ns. To obtain information about the competition of recombination processes involving atomic and molecular ions, pulsed electron "heating" of the decaying plasma was performed. Unlike a similar experiment at significantly higher gas pressure [7], in this experiment, under conditions of relatively slow electron temperature relaxation T_e due to elastic collisions with atoms, it was more expedient to use high-frequency heating technique: in the afterglow, for $\delta t \approx 1$ μs, a high-frequency voltage was applied to the inductance coil wound around the DBD electrodes. The choice of the specified duration δt, much shorter than the characteristic temperature establishment time t_{T_e}, is convenient as it allows to quickly heat the electrons and observe the return of neon atom line intensities to their initial values, thereby estimating the characteristic electron "cooling" time. The sharpness of line intensities' response $J(Te)$ to electron temperature changes indicated the mechanism of excited levels population: for impact-radiative recombination $J(T_e) \propto T_e^{-9/2}$ [8],

while the dissociative recombination flux follows a significantly weaker dependence, close to T_e^{-k} with coefficient k ranging from 3/2 to 1/2 for different ions [9]. Based on the results of such experiment, electron density [e] can also be estimated by analyzing the response of neon atoms population in resonant states $Ne(3_s(^3P_1)(t)$ to changes in T_e [1]. The value [e] in the initial stage of plasma decay was approximately 10^{11} cm^{-3}.

When recording spectra, in addition to the number of periods N_p (i.e., registration time), scanning speed, number of spectrum points, and time intervals (Δt) for photomultiplier signal gating were set.

Characteristic time dependencies of spectral line intensities in discharge and afterglow are shown in Fig. 2. Line segments with arrows indicate the position and duration of gating intervals (Δt) during spectra recording. Configuration levels $2p^53p$ are indicated in Paschen notation. The data in Fig. 2 were obtained at different N_p and therefore do not allow comparison of absolute intensity values. Such comparison for transition lines $3p \rightarrow 3s$ can be made using discharge and afterglow emission spectra recordings shown in Fig. 3 and 4. It is evident that over time, there is a radical change in the relative intensities of some neon lines. Note that the entire time interval in Fig. 2*a*, as will be seen, is less than the characteristic time t_T of electron temperature relaxation due to elastic collisions with atoms, so during the first 30 μs, plasma emission in the atomic spectrum is associated with electron impact excitation. The behavior of ionic lines (we showed it using the example of the 439.2 nm line, transition $4f \rightarrow 3d$, for completeness of the barrier discharge emission pattern) is significantly different.

The high gas purity in the experiment is indicated by the low intensity of the hydrogen line Hα, whose position is marked in Fig. 3*a*. As follows from the data in Fig. 2*b*, recombination population of excited neon atom levels begins at times $t \geqslant 100$ μs and is also accompanied by a noticeable change in the afterglow spectrum over time (Fig. 4). Fig. 2*b* shows the response of neon atom spectral lines to electron heating by RF field pulses. The intensity relaxation rate allows estimating the characteristic electron "cooling" time in this afterglow stage: $t_{T_e} \gg 50$ μs.

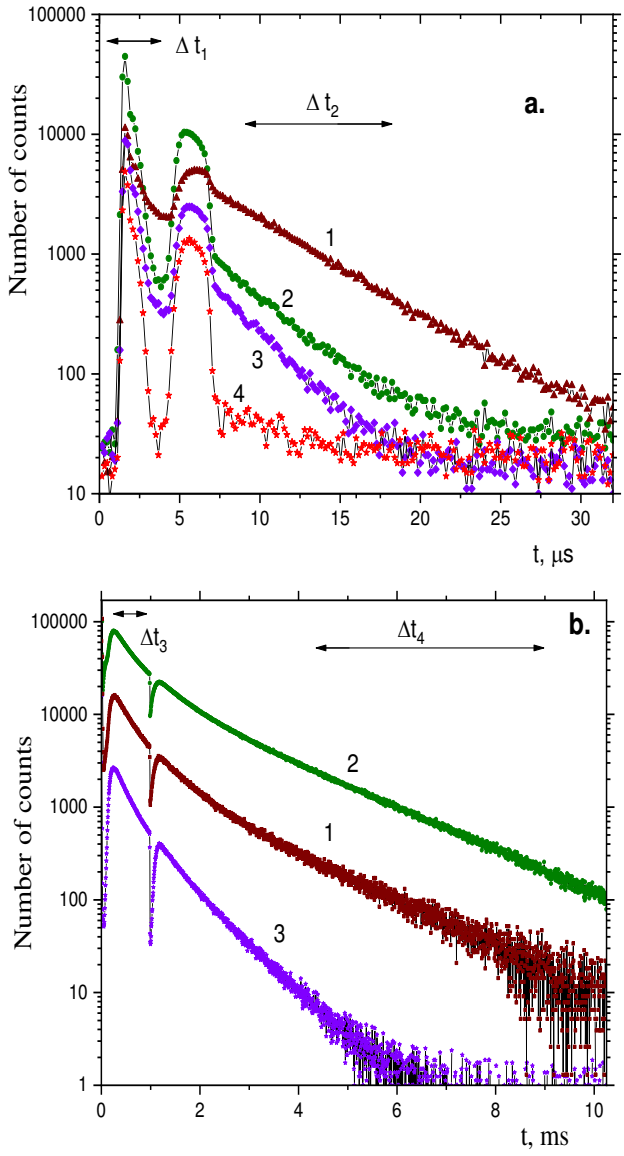

Fig. 2. Spectral line intensities in discharge and early after glow (*a*) and in recombination stage (*b*). *1* – 724.5 nm (upper level $2p_{10}$), *2* — 585.2 nm ($2p_1$), 3 — 576.4 nm (transition $4d \rightarrow 3p$), 4 – ionic line 439.2 nm. $t = 0$– discharge initiation. Neon pressure 1.7 Torr

3. DISCUSSION OF RESULTS

3.1. Electron Excitation

The difference in spectra in Fig. 3 regarding the most indicative changes in relative line intensities can be explained by referring to the research results of direct and stepwise population of 3*p*-levels of neon atom. First, let's point out the ratio $J_{640.2}/J_{585.2}$. The table contains data from [10] about the ratios of direct excitation cross-sections of neon lines and direct excitation cross-sections of levels $2p^53p$ [11] to corresponding values for the 585.2 nm line

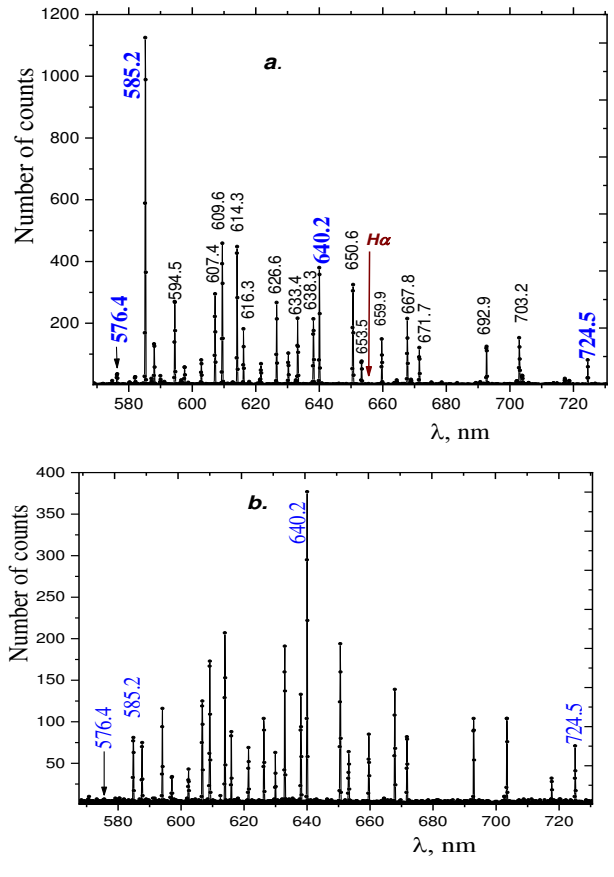

Fig. 3. Discharge emission spectra (*a*) and early afterglow stage (*b*). Gating intervals Δt_1 (a) and Δt_1 (*b*). Lines shown in Fig. 2 or mentioned in the text are highlighted. Hα in Fig.2a – position of hydrogen line Hα

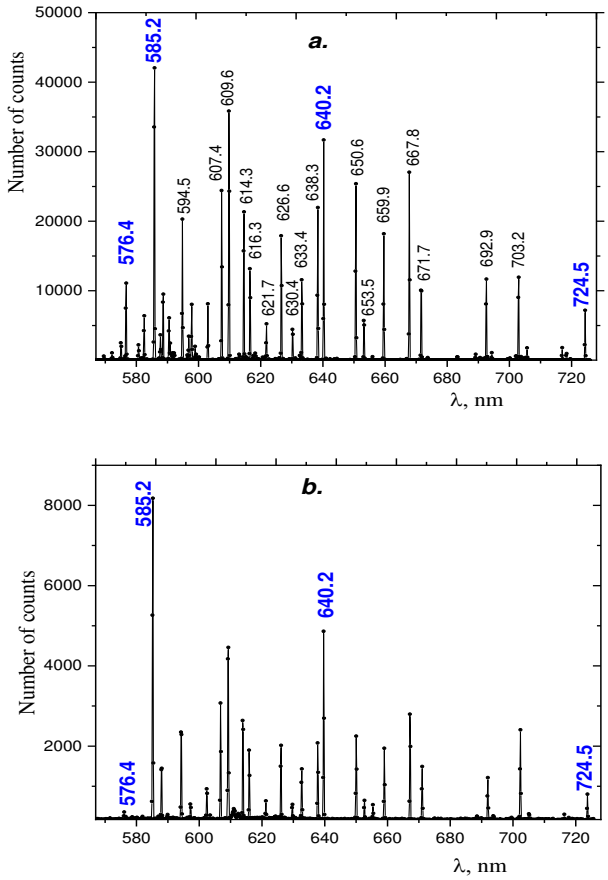

Fig. 4. Spectra of the recombination stage of afterglow. Gating intervals Δt_3 (a) and Δt_4 (b)

(upper level $2p_1$) at electron energy of 30 eV. These data predict maximum brightness of the 585.2 nm line in case of direct excitation of levels from the ground state of neon atom $^1S_0$, which agrees with the line intensity ratios in the spectrum during the gating interval Δt_1 (recalculated according to the sensitivity dependence of the registration scheme $S(\lambda)$ on wavelength and transition probability branching coefficients). Similar changes in spectrum were observed by authors [12] when studying the breakdown mechanism in a long discharge tube filled with neon at pressure P_{Ne} » 1 Torr.

Regarding stepwise excitation, according to [13, 14], the ratio of excitation cross-sections of levels $2p_1$ and $2p_9$ (upper level of 640.2 nm line) from the most populated level $1s_5$ configuration $2p53s1s_5 \rightarrow 2p_9$ and $1s_5 \rightarrow 2p_1$ (optically forbidden transition) is more than 10. The experiment shows the ratio $J_{640.2}/J_{585.2}$ in the spectrum Fig.3*b* (branching coefficients of transition probabilities for levels ($2p_9$ = 1) and $2p_1$ (≈ 0.98) are close) close to the cross-section ratio.

The relationship between stepwise and direct excitation flows of individual levels is equally important for clarifying the excitation mechanism. As can be seen from the data in Fig. 2, after the end of the second half-wave of discharge, the intensity $J_{585.2}$ decreases by an order of magnitude, while $J_{724.5}$ (upper level $2p^{10}$) undergoes only minor changes. Such a difference in the behavior of the 585.2 and 752.4 nm lines agrees with observations [15], according to which the population of level $2p_1$ in discharges is usually more than determined by direct excitation. The authors [15] associate this effect with the difference in excitation cross-sections due to the prohibition of optical transitions to the most populated metastable states $^3P_0$ (level $1s_3$) and $^3P_2$ (level $1s_5$).

It is important to emphasize that the change in the excitation mode of both atomic and ionic levels

after the second half-wave of discharge occurs within less than 0.5 μs. The relaxation rate of the excited level population, provided that its intrinsic radiation time (for example, for $2p_1$ — $1.7 \cdot 10^{-8}$ s [16]) is small compared to the observed changes, is determined by the source parameters, i.e., in this case, by the electron temperature relaxation rate $T_e(t)$ and the accompanying decrease in the $F_D(T_e)$ direct population flux. It is easy to show that the electron temperature balance in discharge and immediately after discharge termination is determined by energy loss during inelastic collisions of electrons with neon atoms, while elastic collisions, which are sufficient to explain phenomena in recombination afterglow, play an insignificant role. To demonstrate this, let's compare the energy spent during the t_d discharge (several μs) on ionization $[e]eV_i$ (for neon $eV_i = 21.56$ eV) and excitation of atoms in metastable $1s_3$, $1s_5$ and resonant $1s_2$, $1s_4$ states with total density close to [e], and energy around 16.5 eV, with electron energy loss during elastic collisions over the same time period $\delta E \approx [e]m_e / M_{\mathrm{Ne}} \nu_{ea} T_e t_d$, where $\nu_{ea} = [\mathrm{Ne}]\nu_e\sigma_e$ is the collision frequency of electrons with neon atoms. Since the electron transport cross-section is small ($\sigma_e \approx 2 \cdot 10^{-16}\mathrm{cm}^2$) and weakly depends on energy [17], such an estimate for neon atom density $[\mathrm{Ne}] \approx 5.5 \cdot 10^{-16}\mathrm{cm}^{-3}$ at temperature T_e of several eV attributes no more than 1/20 fraction of energy loss to elastic collisions. Thus, focusing on $t_{T_e} \gg 50$ s in late afterglow at 1.7 Torr pressure, we estimate the characteristic electron energy relaxation time immediately after discharge termination as $t_{T_e} \gg 2.5$ μs, which qualitatively (considering the near-exponential dependence of direct excitation flux on electron temperature at threshold $E_{th} \gg 18$ eV) explains the steepness of initial intensity decrease of $J_{585.2}(t)$ and other lines in Fig. 2*a*.

Note that when discussing the dependence of the considered process rates on electron temperature, we only address their qualitative nature. The calculation $T_e(t)$ (ideally of the electron energy distribution function) in plasma created by barrier discharge is a complex task requiring, in particular, consideration of the electric field created by charges on the internal surfaces of dielectric walls of the discharge tube near the electrodes. At this level of analysis, we can only assume that, due to the radial symmetry of plasma emission after the creation stage (two half-waves of discharge current of different polarity lasting several microseconds) [2], their influence is small.

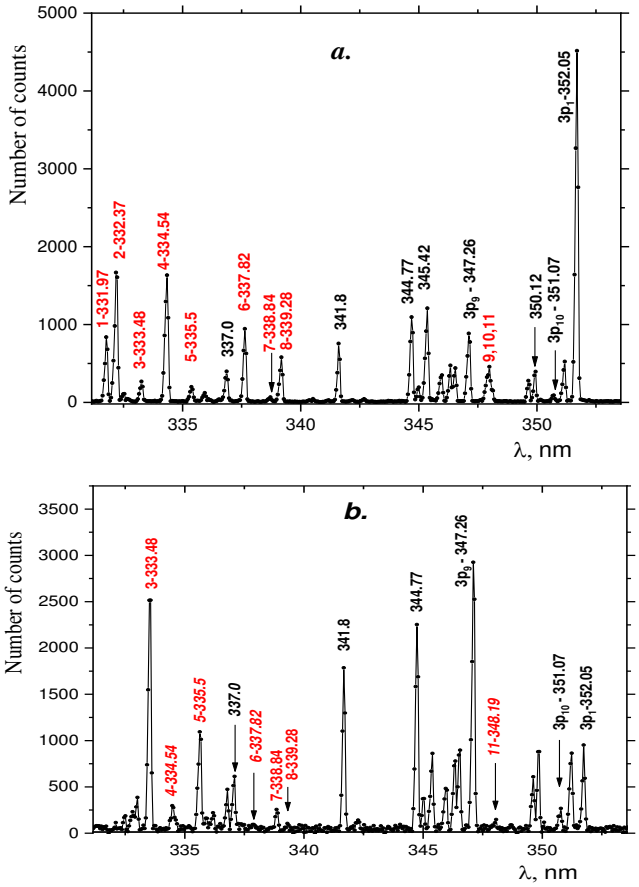

Fig. 5. Direct excitation spectra (*a*, Δt_1) and recombination (*b*, Δt_3) in the near ultraviolet region. Neon pressure 0.4 Torr. Ionic line wavelengths are preceded by numbers from 1 to 11 (for example, 3–333.48 nm)

We conducted similar measurements in the near-ultraviolet region (Fig. 5). It can be seen that the spectrum of the used barrier discharge, usually formed exclusively by transition lines of $4p \to 3s$ neon atom in this wavelength region, contains bright ionic lines. As expected, the transition from direct excitation region of $4p$ levels to stepwise excitation was accompanied by changes in relative line intensities characteristic for the red-yellow spectral region in transitions from levels $3p_1$, $3p_9$ and $3p_{10}$ (Paschen notation). Therefore, in this case, we limited ourselves to comparing excitation flows at times Δt_1 and Δt_3.

3.2. Recombination population stage

Recombination mechanisms of populating excited levels of inert gas atoms have been well studied in numerous investigations (main ones listed in review [9]), including in barrier discharge afterglow [18]. Based on these, we can interpret the difference in spectra in Fig. 4*a* and Fig. 4*b*, from which data it

Table. Intensities of-lines in the spectrum Fig.3, relative to the intensity of 582.5 nm line and ratios of corresponding direct excitation cross-sectionsat electron energy 30 eV and stepwise excitation cross-sectionsfrom metastable state(levelin Paschen notation)

λ, nm	J_λ, Δt_1	σ_d[10, 11]	J_λ, Δt_2	σ_{step}
585.2 ($2p_1$)	1	1	1	1
640.2 ($2p_9$)	0.46	0.4, 0.5	6.2	> 10 [13]
724.5 ($2p_{10}$)	0.37	0.1, 0.3	7	> 10 [14]

is evident that by the beginning of the time inte Δt_4 rvalintensities of lines associated with impact-radiative recombination of ions Ne^+ with electrons, as indicated by strong dependence of intensity on T_e (Fig. 2*b*) (shown on the example of 576.4 nm, the upper level belongs to configuration $2p^5 4d$):

$$Ne^+ + e + e \rightarrow Ne^* + e, \qquad (1)$$

decrease so significantly compared to the transition lines $3p \rightarrow 3s$, that in the plasma spectrum they become barely distinguishable against the background of transitions from configuration levels $2p^5 3p$. And at the same time, the relative intensities of transition lines $3p \rightarrow 3s$ in the late afterglow stage (Δt_4) correlate with the population distribution characteristic of dissociative recombination of molecular ions -levels of neon atom [9]:

$$Ne_2^+ + e \rightarrow Ne^* + Ne. \qquad (2)$$

It should be noted that the faster decay in the afterglow of lines appearing due to (1), despite its incomparably low rate compared to (2), is related not only to the difference in dependencies of the number of acts (1) and (2) on electron density but also to the peculiarities of plasma ion composition [3], developing with the initial condition

$$[Ne_2^+] / [Ne^+] \ll 1$$

and increase over time in the relative density of molecular ions due to conversion during triple collisions

$$Ne^+ + Ne + Ne \rightarrow Ne_2^+ + Ne. \qquad (3)$$

Processes (1), (2) also form the recombination spectrum of transitions $4p \rightarrow 3s$, with the only difference from levels $3p$, that over time, along with the lines carrying the impact-radiation recombination flux (clearly visible on the example of line 576.4 nm, Fig. 4), the lines emitted by the three upper levels of configuration $2p^5 4p$ decay faster. This is due to the specifics of the dissociative recombination process in neon [18], for which these levels, located higher in the energy scale than the ground vibrational level of v ion Ne_2^+ ($v = 0$), become inaccessible in the afterglow and are populated mainly due to process (1). This is the only fundamental difference in the population patterns of levels $3p$ and $4p$ of the neon atom in decaying plasma.

In conclusion, a few words about the ion spectrum. In Fig. 5, we present for the first time data allowing comparison of the ion spectrum excited by shock-radiation recombination of a doubly charged ion

$$Ne^{++} + e + e \rightarrow Ne^{+*} + e, \qquad (4)$$

with the electron impact excitation spectrum well-studied in numerous experiments. In such experiments (a hollow cathode discharge is traditionally used as an excitation source [19]), about 2000 transition lines from excited states with principal quantum numbers up to $n = 8$ [16] have been identified. In experiments with low-pressure barrier discharge during the plasma decay stage, we observed transition lines from states with excitation energies from 30.5 eV up to levels of configuration $2s^2 2p^4 4f$ with excitation energy of about 37.5 eV. Of greatest interest, in our view, is the study of the recombination mechanism of ionic level population. This explains the choice of reduced pressure of 0.4 Torr for spectrum analysis in the short-wavelength region: according to [20, 21] in neon plasma, there exists an effective mechanism for ion conversion

$$Ne^{++} + Ne \rightarrow Ne^+ + Ne^+, \qquad (5)$$

suppression of which significantly reduces the destruction of ions Ne^{++} during the transition time $\Delta t_1 \cap \Delta t_3$.

The nature of changes in relative intensities of some ionic lines with transition from Dt_1 to Dt_3 notably differs from that observed in the atomic spectrum. For example, the neighboring lines in the spectrum Fig. 5*a* 332.37 (brightest according to NIST [16], 31.51 eV) and 333.48 (30.88 eV) change multiple times and in opposite directions; from the trio of similarly bright [16] lines 9, 10, 11 (347.95, 348.07 and 348.19 nm) in the recombination stage, only one is noticeable — 348.19 nm. Even more impressive behavior is demonstrated by the 439.2 nm line (transition $4f$ ® $3d$) — in the recombination maximum its intensity is close to that in the discharge, while in the atomic spectrum this difference is at least an order of magnitude. Interpretation of these phenomena requires substantial expansion of experimental material.

4. CONCLUSION

In the wavelength range of 310-730 nm, the spectral composition and temporal characteristics of radiation in the atomic spectrum of a low-frequency pulsed barrier discharge in low-pressure neon have been studied. Comparison of experimental results with literature data on the mechanisms of excited atom formation indicates their clear separation depending on the observation time relative to the discharge onset. Direct and stepwise electron impact excitation with predominant inelastic collisions in the electron energy balance during the active stage (discharge) and early afterglow is replaced by recombination population, accompanied by the formation of a characteristic maximum in populations of all excited states with a predominant role of collisional-radiative recombination of Ne^+ ions. Analysis of spectrum evolution and progression $J(t)$ together with observation of spectral line intensity response to pulsed electron "heating" by high-frequency field leads to the conclusion that in the final stage of plasma decay, radiation is mainly associated with the mechanism of dissociative recombination of molecular Ne_2^+ ions with electrons, forming a distribution of populations characteristic of this process over a limited set of excited neon atom levels. The presented fragments of the ion spectrum, significantly enriching the transition region $4p \rightarrow 3s$, indicate the potential of barrier discharge in the used configuration for studying the role of doubly charged ions in forming the optical properties of decaying plasma.

REFERENCES

1. V.A. Ivanov. Plasma Sources Sci. Technol., 29, 045022 (2020).
2. V.A. Ivanov. Opt. Spectrosc., 130, 799 (2022).
3. V.A. Ivanov. Opt. Spectrosc., 129, 1104 (2021).
4. U. Kogelschatz. Plasma Chem. Plasma Proc., 23, 1 (2003).
5. V.F. Tarasenko, E.B. Chernov, M.V. Erofeev, M.L. Lomaev, A.N. Panchenko, V.S. Skakun, E.A. Sosnin, D.V. Shitz. Appl. Phys. 69A, 327 (1999).
6. V.A. Ivanov. Opt. Spectrosc., 131, 1537 (2023).
7. V.A. Ivanov., Ju.E. Skoblo. Sov. Phys. JETP, 106, 1704 (1994).
8. A.V. Gurevich, L.P. Pitaevskii. Sov. Phys. JETP, 19 (4), 870 (1964).
9. V.A. Ivanov. Usp. Fiz. Nauk. 162, 35 (1992).
10. L. J. Kieffer. Atomic Data. 1, 121 (1969).
11. J. E. Chilton, M. D. Stewart, Jr., Chun C. Lin.Phys. Rev. A 61, 052608 (2000).
12. A.I. Shishpanov, P.S. Bazhin, V.V. Zaletov. Proceedings of All-Russian Conference "Science SPbU - 2022", p.421 (in Russian).
13. J.B. Boffard, M.L. Keeler, G.A. Piech, L.W. Anderson, C.C. Lin. Phys. Rev. A 64, 032708 (2001).
14. S.S. Baghel, S. Guptal, R. K. Gangwar, R. Srivastava. Plasma Sources Sci. Technol., 28, 115010 (2019).
15. V.M. Donelly. Journal of Physics D: Applied Physics. 37, R217 (2004).
16. NIST Atomic Spectra Database Lines Form [Electronic source]. URL: https://physics.nist.gov/PhysRefData/ASD/ lines form.html.
17. M. Adibzadeh, C.E. Theodosiou. Atomic Data and Nuclear Data Tables. 2005. 91, 8 (2005).
18. S. V. Gordeev, V.A. Ivanov, Yu.E. Skoblo. Opt. Spectrosc., 127, 418 (2019).
19. A.E. Kramida, G. Nave. Eur. Phys. J. D, 39, 331 (2006).
20. F.J. de Hoog, H.J. Oskam. J. Appl. Phys., 44, 3496 (1973).
21. R. Johnsen., M.A. Biondi. Phys. Rev. A, 18 (3), 996 (1978).